Dalton Transactions

Accepted Manuscript

ROYAL SOCIETY OF CHEMISTRY

www.rsc.org/dalton

Dalton Transactions

ARTICLE

Construction of tetranuclear metallacycles based on half-sandwich Ir, Rh fragments and pyridyl-substituted ligands with different coordinate vectors

Received 00th January 2015,
Accepted 00th January 2015

DOI: 10.1039/x0xx00000x

www.rsc.org/

Qi-Jia Fan,[a] Wen-Ying Zhang,[a] Yue-Jian Lin[a] and Guo-Xin Jin*[a]

A series of organometallic macrocycles have been constructed by two-step reactions of [Cp*M(μ-Cl)Cl]$_2$ (M = Ir, Rh), firstly with AgOTf to abstract chloride ions and then with simple pyridyl-substituted ligands pyridyldipyrromethene (H**L^1**), pyridin-4-yl (1H-pyrrol-2-yl)methanone (H**L^2**), pyridine-4-carbohydrazide (H**L^3**), resulting in the formation of the tetranuclear 28-membered metallacycles [(Cp*Ir)(L^1)]$_4$(OTf)$_4$ (**2a**), [(Cp*Rh)(L^1)]$_4$(OTf)$_4$ (**2b**), the 24-membered metallacycles [(Cp*Ir)(L^2)]$_4$ (OTf)$_4$ (**3a**), [(Cp*Rh)(L^2)]$_4$(OTf)$_4$ (**3b**), as well as [(Cp*Ir)(L^3)]$_4$(OTf)$_4$ (**4a**) and [(Cp*Rh)(L^3)]$_4$(OTf)$_4$ (**4b**). Four target complexes were characterised by single crystal X-ray analyses, revealing that these metallacycles constructed from half-sandwich metal corners and pyridyl-substituted linkers form large ring structures. The observed variation in the metallacyclic geometries was explained on the basis of the structural flexibility of the corner fragments, subtle changes in coordination geometries, and changes in the orientation of the coordinate vectors in the given ligands, as well as the dihedral angles between the two binding fragments in the nonplanar ligands.

Introduction

The last two decades have witnessed the rapid development of the synthesis and characterization of transition metal-mediated self-assembled organometallic macrocycles and cages.[1] This particular research field is receiving an increasing amount of attention due to the fact that these supramolecular structures display interesting functional properties and applications in various fields, including host–guest chemistry, redox activity, magnetic behaviour, photo- and electrochemical sensing, and catalysis.[2] Much effort has been devoted to tuning the metallic building blocks or the organic linkers in order to reach the stage of rational design of the exact architectures. Among the building blocks explored, the introduction of rigid organic ligands bearing two different coordination poles as linkers, for example pyridinethiols[3] and pyridyl-substituted imidazole,[4] can impart great versatility of coordination chemistry with metal centers. Ligands such as 2,3-dihydroxypyridine, 3-acetamido-2-hydroxypyridine, 2,3-dihydroxyquinoline, 2,3-dihydroxyquinoxaline, 6-methyl-2,3-phenazinediol, 3,4-dihydroxy-2-methylpyridine and a series of pyridyl substituted β-diketonate ligands, have also been used to great success.[5]

Meanwhile, *half*-sandwich Cp*M (M = Ir, Rh) units with three-legged piano-stool shape frequently act as corners in framework geometries, where the piano stool legs can be variably connected with N-, O-, S-, or P-donor ligands.[6] In this work, our efforts have been focused on finding functional ligands suitable for the construction of new supramolecular organometallic structures, whereby several pyridyl-substituted ligands with two different coordination poles were prepared as relatively rigid bridges, with 170° or nearly 140° bridging angles between the heteroatom group plane and the N-pyridyl connecting atoms. These proligands contain both a monodentate and a chelating binding site, as shown in Figure 1. These ligands have been used as linkers for the construction of one-dimensional coordination polymers,[7] but in this work they are recognised as particularly useful linkages in the construction of large, higher-dimensional ring arrangements. Furthermore, the introduction of these simple units, together with the Cp* ligands, has been demonstrated to be efficient in enhancing the solubility, thermal stabilities, and other factors needed for flexibility in fine-tuning processes.[8]

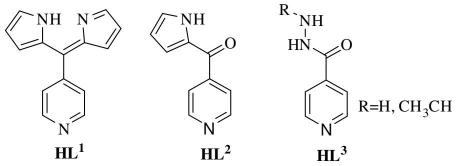

Figure 1 Pyridine-substituted ligands used in this work.

We report herein the synthesis of tetranuclear 28-membered metallacycles **2a** and **2b** with distorted tetrahedral geometries, 24-membered tetranuclear metallacycles **3a**, **3b**, and **4a**, **4b** with distorted parallelogram type geometries (Scheme 1), which were obtained from the two-step reactions of [Cp*M(μ-Cl)Cl]$_2$ (M = Ir, Rh) with initial activation by AgOTf to create labile coordination sites, and then via reaction with the pyridyl-substituted simple proligands (**HL^1**, H**L^2**, H**L^3**). Additionally, the mainly synthetic strategy based on different

---

[a] State Key Laboratory of Molecular Engineering of Polymers, Collaborative Innovation Center of Chemistry for Energy Materials, Department of Chemistry, Fudan University, Shanghai 200433, P. R. China; E-mail: gxjin@fudan.edu.cn

*†Electronic Supplementary Information (ESI) available: CCDC 1440254 (**2a**), 1440255 (**3b**), 1440256 (**4a**) and 1440257 (**4b**) contain the supplementary crystallographic data for this paper.*

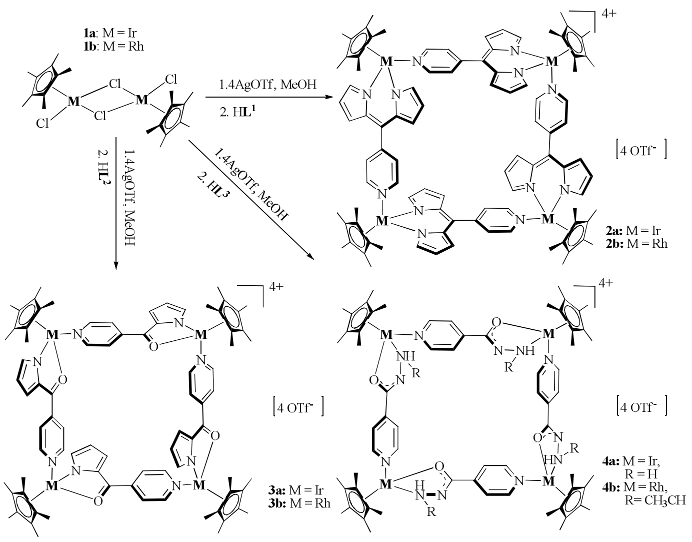

Scheme 1. Synthetic routes to metallacyclic complexes prepared herein.

coordination vectors may provide us the possibility to realise metallacycles with novel structures and properties, and a chance for practical applications.

Results and Discussion

Synthesis and characterisation

As shown in Scheme 1, ligand H**L^1** was prepared according to literature methods.[9] H**L^2** was synthesised through a slightly modified literature procedure.[10] Single crystals of **2a**, **3b**, **4a** and **4b** were obtained by diffusion of ether into their concentrated methanol or methanol/acetonitrile solutions at ambient temperature. Furthermore, the structures of all six target products were confirmed by NMR, IR spectrum and elemental analyses.

The tetranuclear metallacycles 2a and 2b. As can be seen from Scheme 1, [Cp*M(μ-Cl)Cl]$_2$ (M = Ir, Rh) was first treated with more than four equivalents of AgOTf followed by removal of the white AgCl precipitate. Methanol solutions of the proligand H**L^1** were added, providing the desired compounds [(Cp*Ir)(L^1)]$_4$(OTf)$_4$ (**2a**) and [(Cp*Rh)(L^1)]$_4$(OTf)$_4$ (**2b**) after recrystallisation. These products were stable in ambient air. Their IR spectra showed strong bands at approximately 1596 cm^{-1} for **2a** and 1593 cm^{-1} for **2b**, owing to the ν(C=C) stretching of the bridging dipyrromethane ligands. The ^{1}H NMR spectra of **2a** and **2b** in MeOH exhibited a sharp singlet at about δ = 1.60 ppm due to the Cp* protons, **2a** and **2b** pyridyl protons signals were observed as two doublet at 7.52, 8.78 ppm and 7.24, 8.39 ppm, respectively, indicating the typical chemical shift of the pyridyl-substituted dipyrromethane upon metal coordination. Compounds **2a** and **2b** are soluble in MeOH.

The tetranuclear metallacycles 3a and 3b. Mixtures of [Cp*M(μ-Cl)Cl]$_2$ (M = Ir, Rh) and more than four equivalents of AgOTf were stirred at room temperature. After filtration of the AgCl precipitate, methanol solutions of proligand H**L^2** deprotonated with sodium acetate were added to the filtrate. [(Cp*Ir)(L^2)]$_4$(OTf)$_4$ (**3a**) and [(Cp*Rh)(L^2)]$_4$(OTf)$_4$ (**3b**) was obtained after recrystallisation. Their IR spectra showed strong bands at approximately 1600 cm^{-1} assigned to the ν(C=O) stretching vibration of the bridging ketone ligands. The ^{1}H NMR spectra of **3b** in CDCl$_3$ exhibited a sharp Cp* singlet at about δ = 1.63 ppm and pyridyl protons signals were observed as two doublets at 8.81, 7.70 ppm. The ^{1}H NMR spectrum of **3a** is essentially identical. Complexes **3a** and **3b** are soluble in CH$_2$Cl$_2$.

The tetranuclear metallacycles 4a and 4b. [Cp*M(μ-Cl)Cl]$_2$ (M = Ir, Rh) was treated with more than four equivalents of AgOTf, followed by separation of the AgCl precipitate. Subsequent reactions with the proligand H**L^3**, followed by concentration of the reaction solution and recrystallisation, provided the desired crystalline compounds [(Cp*Ir)(L^3)]$_4$(OTf)$_4$ (**4a**) and [(Cp*Rh)(L^3)]$_4$(OTf)$_4$ (**4b**). Their IR spectra showed strong bands at approximately 1495 cm^{-1} for **4a** and 1497 cm^{-1} for **4b**, attributed to the ν(C=O) stretching of the bridging isoniazid ligands. The ^{1}H NMR spectra of **4a** (MeOD) and **4b** (MeOD) exhibited typical signal patterns for the protons of the Cp* ligands and the pyridyl protons.

Description of the molecular structures of complexes.

Detailed structural information of **2a**, **3b**, **4a**, **4b** were obtained from single-crystal X-ray diffraction analyses. For the ligand H**L^1**, we only have a single-crystal structure of **2a**, thus the structure of the crystal of **2a** is discussed in detail as a representative of the two. Perspective drawings of **2a** are shown in Figure 2. As shown in Figures 2b and 2c, the molecular structures revealed a traditional tetranuclear metallacycle possessing a 28-membered inner ring. The four η^5-Cp*M fragments are bridged by four dipyrrin (H**L^1**) ligands. Each metal center is thus coordinated by two adjacent N-dipyrrinato atoms and one N-pyridyl atom, forming the aforementioned three-legged piano stool. Complex **2a** shows crystallographic tetragonal symmetry. The average edge dimension (Ir-dipyrrin-Ir) of the metallacycles is 9.87 Å. In a simplified view, the geometry of the tetranulear metallacycle can be described as a normal tetrahedral structure with slight distortion (Figure 2c). The Ir atoms are located at the four vertices of the tetrahedron with average diagonal lengths of 10.35 Å (Ir1A-Ir1B), and the four edges are occupied by the bridging ligands, resulting in metal-metal-metal angles of 58.395^{o} (Ir1B-Ir1-Ir1C), 58.395^{o} (Ir1-Ir1C-IrA), and 63.210^{o} (Ir1C-Ir1B-Ir1). Furthermore, the dihedral angles between the two binding units in H**L**^{1} is approximately 69^{o}.

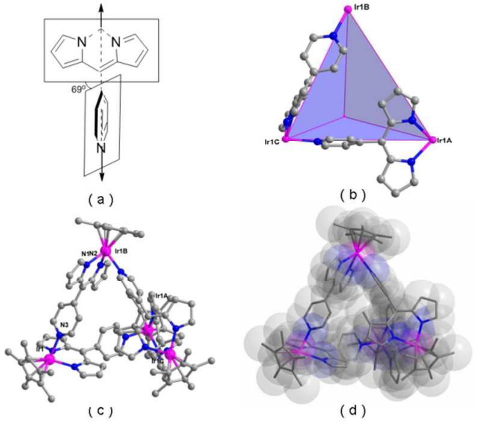

Figure 2. (a) Dihedral angles of the ditopic ligand H**L**^{1}; (b) Compound **2a** can be described as having distorted tetrahedral geometry, in which the metals occupy the vertices, and the pyridine-substituted ligands connect these vertices; (c) Crystallographically-determined molecular structure of the cation of **2a**; (d) View of **2a** in space-filling mode. Triflate anions and non-coordinated solvent molecules, as well as hydrogen atoms, are omitted for clarity. (the graphic is based on the true crystal structure of **2a**. Ir, purple; C, gray; N, blue).

Similar to compound **2a**, compound **3b** also bears units with a three-legged piano stool shape, but in this case, four metals are linked by four 4-pyridinyl-1H-pyrrol-2-ylmethanone ligands (H**L**^{2}) to form a 28-membered inner ring (Figure 3). Perspective drawings of **3b** are shown in Figure 2c. Compound **3b** can be described as having a distorted quadrilateral geometry for clarity (Figure 2c). Each metal centre is located at one of the four vertices of the quadrilateral with the same Rh-L^{2}-Rh edge dimensions of 9.09 Å and Rh-Rh-Rh angles of 83.26^{o}. Four of the quadrilateral edges are occupied by H**L**^{2} ligands to form a folded square in which the distance between the digonal atoms is 12.08 Å. The dihedral angles between the two binding units in H**L**^{2} are approximately 19^{o}.

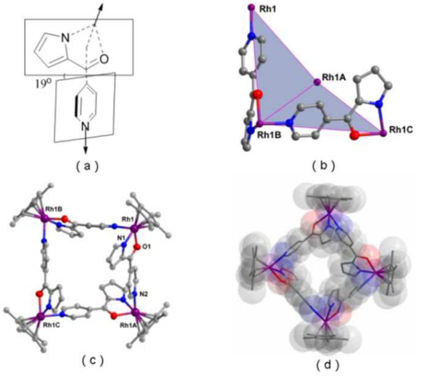

Figure 3. (a) Dihedral angles of the ditopic ligand H**L**^{2}; (b) Compound **3b** can be described as having distorted parallelogram geometry, in which the metals occupy the vertices, and the pyridine-substituted ligands connect these vertices; (c) Crystallographically-determined molecular structure of the cation of **3b**; (d) View of **3b** in space-filling mode. Triflate anions and non-coordinated solvent molecules, as well as hydrogen atoms, are omitted for clarity. (the graphic is based on the true crystal structure of **3b**. Rh, purple; C, gray; O, red; N, blue).

The molecular structures of **4a** and **4b** turned out to be very similar, therefore the structure of compound **4b** is prevailingly discussed. Perspective drawings of **4b** are shown in Figure 4. The four rhodium centers form the four vertices of the parallelogram plane with a 24-membered inner ring. As shown in Figure 4c, compound **4b** shows an average edge length of 9.06 Å, somewhat shorter than the corresponding length in **3b**, as well as M-M-M angles of 83.78^{o}. Four of the parallelogram edges are occupied by H**L**^{3} ligands to form a folded square in which the distance between the digonal atoms is 12.11 Å. It obvious that when coordinated to the metal, the dihedral angles between the two binding units in H**L**^{3} is only 9^{o}.

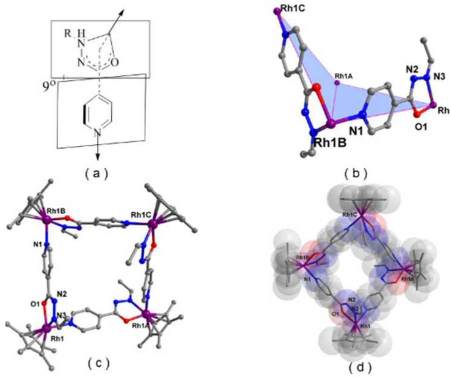

Figure 4. (a) Dihedral angles of the ditopic ligand H**L**^{3}; (b) Compound **4b** can be described as having a distorted parallelogram geometry, in which the metals occupy the vertices, and the pyridine-substituted ligands connect these vertices; (c) Crystallographically-determined molecular structure of the cation of **4b**; (d) View of **4b** in space-filling mode. Triflate anions and non-coordinated solvent molecules, as well as hydrogen atoms, are omitted for clarity. (the graphic is based on the true crystal structure of **4b**. Rh, purple; C, gray; O, red; N, blue).

Although only a little difference in the molecular structures between **4a** and **4b**, we present the structure of **4a** in the following Figure 5b. In this metallacycle the length of C6-O1 is 1.31 Å, and the distance of C6-N1 is 1.28 Å, thus we tend to describe the N1-C6-O1 part as a delocalized system, this can also be consistent with the compound **4b**. To our surprise, N1 may be partial oxidation about 25% of the ratio, we have already describe it in the Figure 5a. And in asymmetric unit of the date of **4a**, there were half of a diethyl ether and a quarter of a water molecule which could not be restrained properly, therefore, SQUEEZE algorithm was used to omit them. Even the structure of **4b**, like compounds **3b**, contains large solvent accessible voids, we are very disappointed to find that there is no solvent molecules in the cavity.

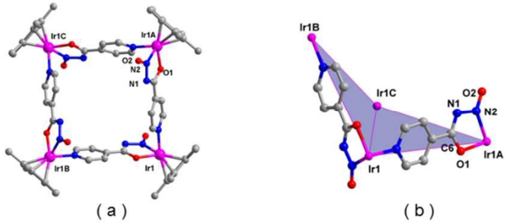

Figure 5. (a) Crystallographically-determined molecular structure of the cation of **4a**; (b) Compound **4a** can be described as having

distorted parallelogram geometry, in which the metals occupy the vertices, and the pyridine-substituted ligands connect these vertices. Triflate anions and non-coordinated solvent molecules, as well as hydrogen atoms, are omitted for clarity. (the graphic is based on the true crystal structure of **4a**. Ir, purple; C, gray; O, red; N, blue).

Self-assembly has become an excellent tool for understanding supramolecular structures, which can further guide the design of molecular self-assembly on the molecular level. After many years of effort, scientists have compiled a number of rules that attempt to explain the laws of self-assembly.[11] In general, both the coordination mode of the metal-containing fragment and the coordination orientation of organic bridging ligands determine the final molecular configuration and size of supramolecular assemblies.[12] The half-sandwich metal corners used in this work preferentially accommodate one bidentate and one monodentate ligand. Raymond and Caulder summarised the ligand coordination mode and direction as the “ligand vector”, greatly simplifying our understanding of molecular assembly.[13] In Ir and Rh half-sandwich macrocyclic compounds, obviously the metallocene ligand bridging angle and vector direction play an important role in the coordination configuration of the resulting macrocyclic compounds. Severin et al. have concluded that, when the angle of the coordinate vector is less than or equal to 90^o, trinuclear metallacycles are often generated, and when the coordinate vector angle is greater than 90^o, tetranuclear metallacycles are often generated.[14]

Among the three ligands we have chosen, the coordinate vector is obviously different. The values of H**L^1**, H**L^2**, H**L^3** are 170^o, 145^o, 142^o, respectively. Furthermore, when considering the dihedral angles between the two binding units in H**L^2** and H**L^1**, the dihedral angle of 19^o is smaller than 69^o, which perhaps has the collateral effect of enforcing the folded-square shape. The several tetranuclear macrocyclic compounds structures we have obtained herein are also consistent with the above rules of Severin and coworkers. It is precisely because of the difference in the coordinate vector, resulting in a slight difference in the degree of twist of the tetranuclear compounds, that their structures range from normal tetrahedral to distorted parallelogram, and the dihedral angles of the complexes are 75^o, 54^o and 52^o, respectively.

Conclusions

In conclusion, a series of half-sandwich iridium and rhodium metal-based tetranuclear metallacycles have been synthesised and characterised, having distorted tetrahedral and parallelogram geometries. Hence, in these metallacyclic compounds the dihedral angles are not the same, which is due to the ligands we have chosen and their differing coordinate vector angles. On the basis of the derived principles for the construction of supramoelcular structures, we are currently attempting to synthesise a series of multinuclear metallacycles with designed properties, with a view towards practical applications based on host-guest behaviour.

Experimental Section

General considerations.

All manipulations were carried out under an atmosphere of nitrogen using standard Schlenk techniques. All of the solvents were freshly distilled prior to use. Dichloromethane and methanol were respectively distilled from CaH_2 or magnesium/I_2. The starting materials [Cp*IrCl(μ-Cl)]$_2$ and [Cp*RhCl(μ-Cl)]$_2$ were prepared according to literature methods.[15] The ligands H**L^1**, H**L^2** and H**L^3** were synthesised according to literature methods or minor modifications thereof. Other chemicals were obtained commercially and used without further purification. Elemental analyses were performed on an Elementar III Vario EI analyzer. ^{1}H NMR (400 MHz) spectra were recorded on a Bruker DMX-500 spectrometer in CD_3OD-D_4 or DMSO-D_6 solution. IR spectra were measured on a Nicolet Avatar-360 spectrophotometer.

Synthesis of complexes 2a and 2b.

To a solution of [Cp*IrCl(μ-Cl)]$_2$ (**1a**, 40 mg, 0.05 mmol) or [Cp*RhCl(μ-Cl)]$_2$ (**1b**, 31.1 mg, 0.05 mmol) in MeOH (15 mL), AgOTf (25.7 mg, 0.11 mmol) was added and the mixture was sheltered from light. After stirring at room temperature for 5 h, the silver salt precipitate was removed by filtering under a nitrogen atmosphere. Solid H**L^1** (14.3 mg, 0.05 mmol) was added to the remaining solution and the mixture was stirred vigorously for 24 h. Later, the solution was concentrated in a rotary evaporator to 3 mL and extracted with diethyl ether (20 mL). The brown products were separated by centrifugation and further dried under vacuum. **2a**, Yield: 23.6 mg, 68%; **2b**, 15.5 mg, 48%. Crystals of **2a** suitable for X-ray diffraction study were obtained by slow diffusion with diethyl ether into MeOH solutions.

Data for complex 2a. Anal. Calcd for $C_{100}H_{100}N_{12}Ir_4O_{12}S_4F_{12}$: C 43.09; H 3.59; N 6.03. Found: C 42.91; H 3.37; N 5.88. ^{1}H NMR (400 MHz, DMSO-D_6): 8.78 (2H, m, -pyridyl), 7.52 (2H, m, -pyridyl), 7.42 (2H, s, =CH), 6.65 (2H, m, =CH), 6.41 (2H, m, =CH), 1.63 (15H, m, -CH_3). IR (KBr, cm^{-1}): 3224 (w), 3101 (w), 3039 (w), 1596 (w), 1584 (w), 1415 (w), 1384 (w), 1354 (w), 1327 (m), 1273 (m), 1252 (m), 1119 (w), 1097 (m), 1047 (m), 1007 (s), 944 (m), 876 (m), 795 (s), 717 (s), 651 (s).

Data for complex 2b. Anal. Calcd for $C_{100}H_{100}N_{12}Rh_4F_{12}O_{12}S_4$: C 49.39; H 3.86; N 6.91. Found: C 49.06; H 3.67; N 6.88. ^{1}H NMR (400 MHz, DMSO-D_6): 8.39 (2H, m, -pyridyl), 7.24 (2H, m, -pyridyl), 7.02 (2H, s, =CH), 6.35 (2H, m, =CH), 6.31 (2H, m, =CH), 1.55 (15H, m, -CH_3). IR (KBr, cm^{-1}): 3228 (w), 3106 (w), 3034 (w), 1593 (w), 1581 (w), 1417 (w), 1388 (w), 1351 (w), 1322 (m), 1270 (m), 1250 (m), 1116 (w), 1093 (m), 1045(m), 1002 (s), 947 (m), 871 (m), 793 (s), 715 (s), 650 (s).

Synthesis of complexes 3a and 3b.

To a solution of [Cp*IrCl(μ-Cl)]$_2$ (**1a**, 40 mg, 0.05 mmol) or [Cp*RhCl(μ-Cl)]$_2$ (**1b**, 31.1 mg, 0.05 mmol) in CH_2Cl_2 (15 mL), AgOTf (25.7 mg, 0.11 mmol) was added and the mixture was sheltered from light. After stirring at room temperature for 5 h, the silver salt precipitate was removed by filtering under a nitrogen atmosphere. Separately, a solution of H**L^2** (8.6 mg, 0.05 mmol) and CH_3COONa (4.92 mg, 0.05 mmol) dissolved in CH_2Cl_2 (15 mL) was stirred for 2h, at which point the mixtures were combined and stirred vigorously overnight. Later, the solution was concentrated in a rotary evaporator to 3 mL and extracted with diethyl ether (20 mL). The yellow products were separated by centrifuge and further dried under vacuum. **3a**, Yield: 17.5 mg, 54%; **3b**, 16.23 mg, 58%. Crystals of **3b** suitable for X-ray diffraction study were obtained by slow layering with n-hexane with a CH_2Cl_2 solution of the complex.

Data for complex 3a. Anal. Calcd for $C_{84}H_{88}Ir_4N_8O_{16}S_4F_{12}$: C 38.91; H 3.39; N 4.32. Found: C 38.72; H 3.57; N 4.66. ^{1}H NMR (400 MHz, $CDCl_3$-D_1): 9.01 (2H, m, -pyridyl), 7.92 (2H, m, -pyridyl), 7.41 (1H, m, =CH), 7.16 (1H, m, =CH), 6.57 (1H, m, =CH), 1.73 (15H, m, -CH_3). IR (KBr, cm^{-1}): 3117 (w), 3066 (w), 3024 (w), 2988 (w), 2925 (w), 2877 (w), 2805 (w), 2684 (w), 1615 (m), 1603 (m), 1544 (m), 1466(w), 1428 (m), 1415 (m), 1395 (s), 1344 (m), 1325 (m), 1266 (w), 1221 (m), 1198 (w), 1143 (m), 1095 (m), 1065 (w), 1047 (m), 1003 (m), 988 (w), 964 (w), 889 (m), 868 (m), 836 (m), 795 (s), 759 (m), 741 (s), 725 (s).

Data for complex 3b. Anal. Calcd for **3b**, $C_{84}H_{88}Rh_4N_8O_{16}S_4F_{12}$: C 45.01; H 4.42; N 5.00. Found: C 44.92; H 4.27; N 4.86. ^{1}H NMR (400 MHz, $CDCl_3$-D_1): 8.81 (2H, m, -pyridyl), 7.70 (2H, m, -pyridyl), 7.22 (1H, m, =CH), 6.90 (1H, m, =CH), 6.39 (1H, m, =CH), 1.63 (15H, m, -CH_3). IR (KBr, cm^{-1}): 3115 (w), 3063 (w), 3026 (w), 2989 (w), 2921 (w), 2875 (w), 2801 (w), 2683 (w), 1612 (m), 1600 (m), 1542 (m), 1465 (w), 1427 (m), 1412 (m), 1392 (s), 1342 (m), 1320 (m), 1263 (w), 1220 (m), 1197 (w), 1140 (m), 1093 (m), 1064 (w), 1045 (m), 1002 (m), 986 (w), 962 (w), 887 (m), 866 (m), 834 (m), 792 (s), 757 (m), 738 (s), 723 (s).

Synthesis of complexes 4a and 4b.

To a solution of $[Cp^*IrCl(\mu\text{-}Cl)]_2$ (**1a**, 40 mg, 0.05 mmol) or $[Cp^*RhCl(\mu\text{-}Cl)]_2$ (**1b**, 31.1 mg, 0.05 mmol) in MeOH (15 mL), AgOTf (25.7 mg, 0.11 mmol) was added and the mixture was sheltered from light. After stirring at room temperature for 5 h, the silver salt precipitate was removed by filtering under a nitrogen atmosphere. Solid **HL^3** (14.3 mg, 0.05 mmol) was added to the remaining solution and the mixture was stirred vigorously for 12 h. Later, the solution was concentrated in a rotary evaporator to 5 mL and extracted with diethyl ether (20 mL). The yellow products were separated by centrifugation and further dried under vacuum. **4a**, Yield: 18.3 mg, 60%; **4b**, 14.6 mg, 56%. Crystals of **4a** and **4b** suitable for an X-ray diffraction study were obtained by slow diffusion of diethyl ether into a MeOH solution of the complex.

Table 1 Crystallographic data and structure refinement parameters

	2a	**3b**	**4a**	**4b**
formula	$C_{100}H_{100}N_{12}Ir_4O_{12}S_4F_{12}$	$C_{84}H_{88}Rh_4N_8O_{16}S_4F_{12}$	$C_{76}H_{104}F_{12}Ir_4N_{12}O_{20}S_4$	$C_{76}H_{92}F_{12}N_{12}O_{16}Rh_4S_4$
Mr	2786.9	2233.5	2630.7	2197.4
crystal system	Tetragonal	Tetragonal	Tetragonal	Tetragonal
space group	*P 42/n*	*P 42/n*	*P 42/n*	*P 42/n*
a [Å]	18.9052(16)	19.927(3)	20.111(2)	20.036(3)
b [Å]	18.9052(16)	19.927(3)	20.111(2)	20.036(3)
c [Å]	16.5315(14)	12.252(2)	12.1229(19)	12.234(2)
$\alpha/\beta/\gamma$ [º]	90	90	90	90
V [$Å^3$]	5908.5(11)	4865.1(19)	4903.4(13)	4911.4(18)
T [K]	173(2)	173(2)	173(2)	173(2)
Z	2	2	2	2
ρ_{calcd} [g cm^{-3}]	1.567	1.525	1.772	1.486
μ [mm^{-1}]	4.637	0.839	5.585	0.830
F(000)	2720	2256	2556	2224
independent reflections	0.0933	0.0941	0.0821	0.0566
data/restraints/parameters	6439/114/255	5432/6/294	5548/29/267	5642/6/286
R_1/wR_2 [$I > 2\sigma(I)$][a]	0.0929/0.2609	0.0647/0.1512	0.0551/0.1500	0.0576/0.1611
R_1/wR_2 (all data)[a]	0.1565/0.3038	0.1560/0.1845	0.1005/0.1681	0.0869/0.1768
goodness-of-fit	0.979	0.903	0.946	1.037
largest residuals [e $Å^{-3}$]	2.948/-1.718	0.852/-0.424	2.640/-1.761	1.293/-0.756
ρ_{calcd} [g cm^{-3}]	1,231	1.525	1.660	1.486
μ [mm^{-1}]	4.529	0.839	5.578	0.830

[a] $R_1 = \Sigma||F_o| - |F_c||$ (based on reflections with $Fo^2 > 2\sigma F^2$); $wR_2 = \{\Sigma[\omega(Fo^2 - Fc^2)^2]/\Sigma[\omega(Fo^2)^2]\}^{1/2}$; $w = 1/[\sigma^2F0^2 + (0.095P)^2]$; $P = [\max(Fo^2, 0) + 2Fc^2]/3$ (also with $Fo^2 > 2\sigma F^2$

Data for complex 4a. Anal. Calcd for $C_{76}H_{106}F_{12}Ir_4N_{12}O_{19}S_4$: C 34.70; H 3.98; N 6.39. Found: C 34.38; H 3.81; N 6.18. ^{1}H NMR

(400 MHz, DMSO-D_6): 8.87 (2H, m, -pyridyl), 8.46 (2H, m, -pyridyl), 1.69 (15H, m, -CH_3). IR (KBr, cm^{-1}): 2929 (s), 1495 (s), 1388 (s), 1259(w), 1165 (s), 1034 (s), 643 (s), 520 (s).

Data for complex 4b. Anal. Calcd for $C_{76}H_{92}F_{12}Rh_4N_{12}O_{16}S_4$: C 41.50; H 4.19; N 7.64. Found: C 41.27; H 4.21; N 7.38. ^{1}H NMR (400 MHz, DMSO-D_6): 8.99 (2H, m, -pyridyl), 8.56 (2H, m, -pyridyl), 1.63 (15H, m, -CH_3). IR (KBr, cm^{-1}): 2926 (s), 1497 (s), 1385 (s), 1258 (w), 1161 (s), 1031 (s), 639 (s), 518 (s).

Single-Crystal X-ray Structure Determination.

All single crystals were immersed in mother solution and sealed in thin-walled glass. Data were collected on a CCD-Bruker SMART APEX system. All the determinations of unit cell and intensity data were performed with graphite monochromated Mo K_α radiation (λ= 0.71073 Å). All the data were collected at −100 °C using the ω scan technique. The structures were solved by direct methods, using Fourier techniques, and refined on F^2 by a full-matrix least-squares method. All the calculations were carried out with the SHELXTL program. A summary of the crystallographic data and selected experimental information are given in Table 1.

Acknowledgements

This work was supported by the National Science Foundation of China (21531002, 21374019), the Program for Changjiang Scholars and Innovative Research Team in University (IRT-15R12), the National Basic Research Program of China (2015CB856600) and the Shanghai Science Technology Committee (13JC1400600, 13DZ2275200).

References

1. (*a*) S. Leininger, B. Olenyuk and P. J. Stang, *Chem. Rev.*, 2000, **100**, 853; (*b*) S. R. Seidel and P. J. Stang, *Acc. Chem. Res.*, 2002, **35**, 972; (*c*) E. Zangrando, M. Casanova and E. Alessio, *Chem. Rev.*, 2008, **108**, 4979; (*d*) Y. -F. Han, W. -G. Jia, W. -B. Yu and G. -X. Jin, *Chem. Soc. Rev.*, 2009, **38**, 3419; (*e*) T. R. Cook, Y. -R. Zheng and P. J. Stang, *Chem. Rev.*, 2012, **113**, 734; (*f*) S. -L. Huang, Y. -J. Lin, T. S. A. Hor and G. -X. Jin, *J. Am. Chem. Soc.* 2013, **135**, 8125; (*g*) Y.-Y. Zhang, X. -Y. Shen, L. -H. Weng and G. -X. Jin, *J. Am. Chem. Soc.*, 2014, **136**, 15521.
2. (*a*) P. Thanasekaran, R. T. Liao, Y. H. Liu, T. Rajendran, S. Rajagopal and K. L. Lu, *Coord. Chem. Rev.*, 2005, **249**, 1085; (*b*) U. Rosenthal, V. V. Burlakov, M. A. Bach and T. Beweries, *Chem. Soc. Rev.*, 2007, **36**, 719; (*c*) E. Pardo, R. Carrasco, R. R. Garcia, M. Julve, F. Llort, M. C. Munoz, Y. Journaux, E. Ruiz and J. Cano, *J. Am. Chem. Soc.*, 2008, **130**, 576; (*d*) Y.-T. Chan, X.-P. Li, J. Yu, G. A. Carri, C. N. Moorefield, G. R. Newkome and C. Wesdemiotis, *J. Am. Chem. Soc.*, 2011, **133**, 11967; (*e*) T. Jacobs, G. O. Lloyd, J. Gertenbach and K. K. Müller-Nedebock, *Angew. Chem., Int. Ed.*, 2012, **51**, 4913; (*f*) J. K. Cherutoi, J. D. Sandifer, U. R. Pokharel, F. R. Fronczek, S. Pakhomova, and A. W. Maverick, *Inorg. Chem.*, 2015, **54**, 7791.
3. (*a*) S. Onaka, M. Yaguchi, R. Yamauchi, T. Ozeki, M. Ito, T. Sunahara, Y. Sugiura, M. Shiotsuka, K. Nunokawa, M. Horibe, K. Okazaki, A. Iida, H. Chiba, K. Inoue, H. Imai and K. Sako, *J. Organomet. Chem.*, 2005, **690**, 57; (*b*) M. T. Raisanen, N. Runeberg, M. Klinga, M. Nieger, M. Bolte, P. Pyykko, M. Leskela and T. Repo, *Inorg. Chem.*, 2007, **46**, 9954; (*c*) K. Yamanari, I. Fukuda, T. Kawamoto, Y. Kushi, A. Fuyuhiro, N. Kubota, T. Fukuo and R. Arakawa, *Inorg. Chem.*, 1998, **37**, 5611.
4. (*a*) X. Li, B.-L. Wu, C.-Y Niu, Y.-Y. Niu and H.-Y. Zhang, *Cryst. Growth Des.* 2009, **9**, 3423; (*b*) X. -M. Jing, L.-R. Zhang, T.-L. Ma, G.-H. Li, Y. Yu, Q. -S. Huo, M. Eddaoudi and Y. L. Liu, *Cryst. Growth Des.*, 2010, **10**, 492; (*c*) X. -M. Jing,; H. Meng, G. H. Li, Y. Yu, Q. -S. Huo, M. Eddaoudi and Y. -L. Liu, *Cryst. Growth Des.* 2010, **10**, 3489.
5. (*a*) Z. Grote, R. Scopelliti and K. Severin, *J. Am. Chem. Soc.*, 2004, **126**, 16959; (*b*) K. Severin, *Chem. Commun.*, 2006, 3859; (*c*) S. Mirtschin, E. Krasniqi, R. Scopelliti and K. Severin, *Inorg. Chem.*, 2008, **47**, 4454; (*d*) G.-L. Wang, Y.-J. Lin, H. Berke and G.-X. Jin, *Inorg. Chem.*, 2010, **49**, 2193; (*f*) G.-L. Liu, Z.-F. Ju, D.-Q.Yuan, and M.-C. Hong, *Inorg. Chem.*, 2013, **52**, 13815.
6. (*a*) Y.-F. Han, W.-G. Jia, Y.-J. Lin and G.-X. Jin, *Angew. Chem., Int. Ed.*, 2009, **48**, 6234; (*c*) G.-L. Wang, Y.-J. Lin, O. Blacque, H. Berke and G.-X. Jin, *Inorg. Chem.*, 2008, **47**, 2940.
7. (*a*) B. Chen, F. R. Fronczek and A. W. Maverick, *Chem. Commun.*, 2003, **17**, 2166; (*b*) Y. Zhang, B. Chen, F. R. Fronczek and A. W. Maverick, *Inorg. Chem.*, 2008, **47**, 4433; (*c*) B. Chen, F. R. Fronczek and A. W. Maverick, *Inorg. Chem.*, 2004, **43**, 8209; (*d*) V. D. Vreshch, A. B. Lysenko, A. N. Chernega, J. A. K. Howard, H. Krautscheid, J. Sieler and K. V. Domasevitch, *Dalton. Trans.*, 2004, **18**, 2899.
8. (*a*) Y.-F. Han, Y.-J. Lin, W.-G. Jia and G.-X. Jin, *Dalton. Trans.*, 2009, 2077; (*b*) Y. -F. Han and G. -X. Jin, *Chem. Soc. Rev.*, 2014, **43**, 2799.
9. (*a*) S. R. Halper and S. M. Cohen, *Angew. Chem., Int. Ed.*, 2004, **43**, 2385; (*b*) M. Boccalon, E. Lengo, and P. Tecilla, *J. Am. Chem.Soc.*, 2012, **134**, 20310; (*c*) S. R. Halper, L. Do, J. R. Stork and S. M. Cohen, *J. Am. Chem. Soc.*, 2006, **128**, 15255; (*d*) A. Béziau, S. A. Baudron, A. Fluck and M. W. Hosseini, *Inorg. Chem.*, 2013, **52**, 14439.
10. L.-H. Li, G. J. Clarkson, M. R. Lees, S. E. Howson, S.-Y. Tan, S. S. Turner and P. Scott, *Organometallics*, 2015, **34**, 2543.
11. M. Fujita, M. Tominaga, A. Hori and B. Therrien, *Acc. Chem. Res.*, 2005, **38**, 369.
12. K. Severin, Coord. Chem. Rev., 2003, **245**, 3−10; (b) T. R. Cook, V. Vajpayee, M. H. Lee, P. J. Stang and K. W. Chi, *Acc. Chem. Res.*, 2013, **46**, 2464.
13. D. L. Caulder and K. N. Raymond, *Acc. Chem. Res.*, 1999, **32**, 975.
14. M. L. Lehaire, R. Scopelliti, L. Herdeis, K. Polborn, P. Mayer and K. Severin, *Inorg. Chem.*, 2004, **43**, 1609.
15. C. White, A. Yates and P. M. Maitlis, *Inorg. Synth.* 1992, **29**, 228.

Toc Graphic

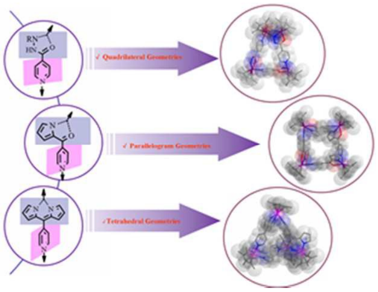

Text:

Two-step reactions of $[Cp^*M(\mu\text{-}Cl)Cl]_2$ (M = Ir, Rh), first with AgOTf and then pyridyl-substituted ligands of different coordinate vectors, resulted in the formation of distorted tetrahedral and parallelogram type tetranuclear metallacycles, respectively.